

## A GEOLOGICAL PERSPECTIVE ON THE USE OF Pb ISOTOPES IN ARCHAEOMETRY\*

F. ALBARÈDE,<sup>1,2</sup> A.-M. DESAULTY<sup>1</sup> and J. BLICHERT-TOFT<sup>1,2</sup>

<sup>1</sup>Ecole Normale Supérieure de Lyon, Université Claude Bernard-Lyon 1, and CNRS, 69007 Lyon, France

<sup>2</sup>Rice University, Department of Earth Science, Houston, TX 77005, USA

*Lead isotope ratios in ore bodies and magmatic rocks depend in a complex way on several a priori independent parameters, including the geological age of the tectonic province in which the ores and magmas formed and its U/Pb ( $\mu$ ) and Th/U ( $\kappa$ ) ratios, two very sensitive parameters characteristic of metal sources. All these parameters are entangled in hard-to-read Pb isotopic ratios. With respect to the commonly used fingerprinting techniques, which rely on the comparison of raw isotope ratios, the main motivation for the present work is to provide a method for making geologically and geochemically educated guesses about metal provenance even in the absence of isotopic data on reference ores. It shows how to unscramble a geological model age and  $\mu$  and  $\kappa$  information from isotopic measurements. This approach brings to light a new organization of the Pb isotope database and an untapped wealth of information that can be used for provenance studies and other archaeometric purposes. We provide expressions with which to calculate these parameters and, using literature data, demonstrate how Pb isotopes in ores and magmas define clear zones in the silver-rich provinces of the Central Andes. We further show how the geological model age and  $\mu$  and  $\kappa$  values fingerprint production areas in 16th–18th century silver coins minted in Mexico and South America. Finally, we use Pb isotopes to illustrate how the Reconquista of the Emirate of Granada (1482–91) and the seizure of the Betic silver mines are reflected in the silver coins of the Catholic Monarchs.*

**KEYWORDS:** ARCHAEOMETRY, Pb ISOTOPES, SPANISH AMERICAS, SPAIN

### INTRODUCTION

The relative abundances of the four Pb isotopes vary because their respective progenitors are different: <sup>204</sup>Pb has no extant progenitor, <sup>206</sup>Pb and <sup>207</sup>Pb are produced by the radioactive decay of <sup>238</sup>U ( $T_{1/2} = 4.47 \text{ Ga}^{-1}$ ) and <sup>235</sup>U ( $T_{1/2} = 0.704 \text{ Ga}^{-1}$ ), respectively, while <sup>208</sup>Pb is produced by the radioactive decay of <sup>232</sup>Th ( $T_{1/2} = 14.0 \text{ Ga}^{-1}$ ). This group of chronometers is described by an apparently simple set of equations and associated graphic representations, yet not simple enough for its legacy to not involve some particularly heated controversies (Ulrych 1967; Oversby and Gast 1968; Gale 1972; Tera and Wasserburg 1972, 1973). In other words, understanding how Pb isotopes ‘work’ is not just a simple matter.

Trace elements have long been used to assess possible origins of historical and archaeological artefacts. Colonial Potosi silver coins, for example, are known to contain less gold (Gordus and Gordus 1981) and more indium (Le Roy Ladurie *et al.* 1990) than silver coins of similar age but different provenance, from Mexico in particular. The relationships between trace element concentrations remain, however, largely descriptive and offer little correspondence with the particular geological backgrounds of the ores in question. In this context, Pb isotopes constitute a superior

\*Received 17 May 2011; accepted 26 August 2011

© University of Oxford, 2011

provenance tool because, contrary to trace element abundances, their variations are rooted in the local geological history, they are not affected by weathering and, due to the small range of atomic numbers, they are essentially immune to modifications by metallurgical processes. The way in which Pb isotopes are used for archaeometric applications consists of straightforward comparison of a set of isotopic ratios, obtained from a database, between a given artefact and ores, or between individual artefacts (e.g., Stos-Gale 2001). The widespread use of Pb isotope compositions as a provenance tool for archaeological artefacts, the emergence of Pb isotope databases conceived specifically for archaeological purposes (Stos-Gale *et al.* 1995; Stos-Gale and Gale 2009), and the lack of modern comprehensive reviews of the theory behind the systematics and use of Pb isotopes crucially emphasize the under-exploitation of Pb isotope data in the context of the geological backgrounds in which the ores used for metallurgy are found. Lead isotopes, and in particular the model ages  $T$  derived from Pb isotope ratios, are useful for fingerprinting the tectonic ages of the geological sources of the ores; for example, the young circum-Mediterranean Alpine belts (<90 Ma) versus the older Hercynian (~300 Ma old) basement of the European Atlantic façade (Desaulty *et al.* 2011). They also can distinguish geological provinces with high  $^{238}\text{U}/^{204}\text{Pb}$  ( $\mu$ ) ratios from those with low  $\mu$ , and likewise tell apart geological provinces with high and low  $^{232}\text{Th}/^{238}\text{U}$  ( $\kappa$ ) ratios,  $\mu$  and  $\kappa$  being two highly characteristic geochemical parameters of metal sources. Because all of these variables are entwined in hard-to-read isotopic ratios of Pb, a major motivation for the present work is to show that unscrambling the geological age and the  $\mu$  and  $\kappa$  values from isotopic measurements brings to light a new organization of the Pb isotope database and an untapped wealth of information that can be used for archaeometric purposes.

The goal of the present work is to show how to make geologically educated guesses on the provenance of artefacts even when data on reference ores are not available. Here, we review the basic sets of equations describing Pb isotope evolution and explain how the parameters relevant to the evolution of a particular ore can be understood. We first show that the set of Pb isotope ratios used for archaeometry ( $^{207}\text{Pb}/^{206}\text{Pb}$ ,  $^{208}\text{Pb}/^{206}\text{Pb}$ ,  $^{204}\text{Pb}/^{206}\text{Pb}$ ) is far from optimal. We then proceed to demonstrate how geological parameters can be extracted from any Pb isotope composition and how these in turn can be used in their own right to identify metal sources. We use as an example a case study of South America made possible by the compilation of Pb isotope compositions in ore deposits and lavas by Mamani *et al.* (2008). We finally provide two examples of the application of Pb isotopes to silver coins as a spin-off from the work by Desaulty *et al.* (2011), which pertain to the fingerprinting of colonial silver in 16th–18th century Spanish America and the monetary imprint of the Reconquista in late 15th century Spain.

#### WHY USE $T$ - $\mu$ - $\kappa$ REPRESENTATION INSTEAD OF RAW ISOTOPIC PLOTS?

Measured lead isotope ratios are directly used for the characterization of metal artefacts, such as coins and tools, and to assign the metals these artefacts were made of to specific ore fields (provenance studies). The choice of ratios used was motivated not by a particular interpretative property, but by the difficulty that has prevailed until this past decade in measuring accurately the less abundant isotope  $^{204}\text{Pb}$ . Plots of  $^{207}\text{Pb}/^{206}\text{Pb}$  versus  $^{208}\text{Pb}/^{206}\text{Pb}$  are therefore prevalent, even in the most recent archaeometry literature (e.g., Ponting *et al.* 2003; Klein *et al.* 2004; Pollard 2008; Cattin *et al.* 2009; Stos-Gale and Gale 2009). It is well known in the geochemical literature, however, that in these plots, modern magmatic and ore provinces tend to form very narrow alignments, which, in addition, tend to overlap strongly with each other (e.g., Blichert-Toft *et al.* 2005) and therefore have limited resolution. The ambiguities resulting from such tight correlations obscure relationships between samples and explain why these plots have found only little

use in geochemistry. With advancing techniques, plots involving  $^{204}\text{Pb}$  have recently found more applications (e.g., Stos-Gale 2001; Baker *et al.* 2005), in particular those using  $^{206}\text{Pb}/^{204}\text{Pb}$  or its reciprocal  $^{204}\text{Pb}/^{206}\text{Pb}$ .

Contrary to isotopic plots, the  $T$ - $\mu$ - $\kappa$  representation explores a three-dimensional space of independent geological parameters. The model age  $T$  is a geochemical measure of the geological age of the province in which ores are found. Because of the simple assumptions involved, the values of  $T$  are not meant to stand for accurate geological dates, but model ages usually are precise enough to identify provinces by their tectonic formation ages. Model ages have been used in archaeometry (Pernicka *et al.* 1993), but only rarely, and their use currently seems to have fallen into oblivion for reasons that still need to be made explicit.  $\mu$  is a measure of how U and Pb separated through time in each geological province: its metamorphic and hydrothermal history may be complex, but—as shown by, for example, the isotopic analysis of Pb in sulphides and K-feldspar in Europe (Michard-Vitrac *et al.* 1981; Bielicki and Tischendorf 1991) and South America (Mamani *et al.* 2008)— $\mu$  zoning is strong and robust (see below).  $\kappa$  varies little, and for geological reasons that are not fully understood. It is likely, however, that the mantle Th/U ratio has varied through geological time, presumably because of the evolving oxidation state of uranium (Elliott *et al.* 1999) and, therefore, that  $\kappa$  reflects the dynamic history of the continental province in which ores are found.

In principle, there should be full correspondence (mapping) between a set of two plots of isotopic ratios, typically combining  $^{207}\text{Pb}/^{206}\text{Pb}$  versus  $^{208}\text{Pb}/^{206}\text{Pb}$  with  $^{207}\text{Pb}/^{206}\text{Pb}$  versus  $^{204}\text{Pb}/^{206}\text{Pb}$ , and the  $T$ - $\mu$ - $\kappa$  representations. Each of the plots of raw isotopic ratios alone only maps two dimensions and it takes a set of three plots to map three dimensions. The literature shows that a straightforward comparison of raw isotopic ratios between specific artefacts and ores may be efficient in particular cases—although with the caveat that the  $^{207}\text{Pb}/^{206}\text{Pb}$  versus  $^{208}\text{Pb}/^{206}\text{Pb}$  plot has little resolution—but it is not geologically informed. Age information is particularly worthy, because a quick inspection of model ages  $T$  immediately signals the origin of ores in ‘Alpine’, ‘Hercynian’, ‘Cordilleran’ and other geological provinces. Variations in  $\mu$  and  $\kappa$  help discriminate segments within geological provinces. The full extent of a three-dimensional  $T$ - $\mu$ - $\kappa$  parameter space and its meaningful coordinates bring genuine geological information that a blind comparison of raw isotopic ratios convolves in an almost irretrievable way. The cost of using the  $T$ - $\mu$ - $\kappa$  coordinates is, of course, the relative complexity of parameter calculation, and the next section will provide some guidelines for how these calculations can be effected.

#### Pb ISOTOPE BASICS

Although case studies will eventually use ages derived from two-stage, closed-system models describing the evolution of Pb isotopes, the so-called one-stage evolution is a preliminary but demonstrative reference. Let us assume that Pb in sample  $i$  evolved from geological age  $T_0$  until today, and use  $x$  for  $^{206}\text{Pb}/^{204}\text{Pb}$ ,  $y$  for  $^{207}\text{Pb}/^{204}\text{Pb}$ , and  $z$  for  $^{208}\text{Pb}/^{204}\text{Pb}$ , with parameters  $\mu = ^{238}\text{U}/^{204}\text{Pb}$  and  $\kappa = ^{232}\text{Th}/^{238}\text{U}$  extrapolated to the present time (e.g., Dickin 2005; Allègre 2008):

$$\begin{aligned}x_i &= x_0 + \mu(e^{\lambda T_0} - 1) \\y_i &= y_0 + \frac{\mu}{137.88}(e^{\lambda T_0} - 1) \\z_i &= z_0 + \mu\kappa(e^{\lambda T_0} - 1)\end{aligned}\tag{1}$$

in which  $\lambda$ ,  $\lambda'$  and  $\lambda''$  stand for the decay constants of  $^{238}\text{U}$ ,  $^{235}\text{U}$  and  $^{232}\text{Th}$ , respectively. The subscript 0 indicates the value of a variable at  $T = T_0$ . Substituting:

$$y_i = y_0 + (x_i - x_0)s(T_0, 0) \quad (2)$$

$$z_i = z_0 + \kappa(x_i - x_0) \times \frac{e^{\lambda''T_0} - 1}{e^{\lambda T_0} - 1} \quad (3)$$

where the slope  $s(T_0, T)$  is given by

$$s(T_0, T) = \frac{1}{137.88} \frac{e^{\lambda T_0} - e^{\lambda T}}{e^{\lambda T_0} - e^{\lambda T}} \quad (4)$$

The ratios  $^{207}\text{Pb}/^{206}\text{Pb}$  ( $y/x$ ) and  $^{208}\text{Pb}/^{206}\text{Pb}$  ( $z/x$ ) most familiar to archaeometrists may now be evaluated as follows:

$$(y/x)_i = \frac{1}{137.88} \frac{e^{\lambda T_0} - 1}{e^{\lambda T_0} - 1} + \left( y_0 - \frac{x_0}{137.8} \frac{e^{\lambda T_0} - 1}{e^{\lambda T_0} - 1} \right) \times \frac{1}{x_i} \quad (5)$$

$$(z/x)_i = \kappa \frac{e^{\lambda''T_0} - 1}{e^{\lambda T_0} - 1} + \left( z_0 - \kappa x_0 \frac{e^{\lambda''T_0} - 1}{e^{\lambda T_0} - 1} \right) \times \frac{1}{x_i} \quad (6)$$

These expressions show that, for different values of  $\mu$  and given values of  $T_0$  and  $\kappa$ ,  $^{207}\text{Pb}/^{206}\text{Pb}$  and  $^{208}\text{Pb}/^{206}\text{Pb}$  vary linearly with  $1/x_i = ^{204}\text{Pb}/^{206}\text{Pb}$  (but not with  $^{206}\text{Pb}/^{204}\text{Pb}$ ) and vary linearly with each other. For mixtures of lead, the same ratios also provide linear relationships. Equations in which the isotope used as the *denominator* is identical for the variables therefore provide linear relationships between the variables.

For the sake of understanding ore deposits, it is often convenient to describe the evolution of a geological object, typically a rock or an ore deposit, as if it has evolved in two stages, labelled 1 and 2, with evolution starting at  $T_0$  (the age of the Earth or a more appropriate old age) and with fractionation of U from Pb; for example, through magmatic or hydrothermal activity, at age  $T_i$ . The present-day values of  $^{206}\text{Pb}/^{204}\text{Pb}$ ,  $^{207}\text{Pb}/^{204}\text{Pb}$  and  $^{208}\text{Pb}/^{204}\text{Pb}$  for a two-stage evolution read as follows:

$$\begin{aligned} x_i &= x_0 + \mu_1(e^{\lambda T_0} - e^{\lambda T_i}) + \mu_2(e^{\lambda T_i} - 1) \\ y_i &= y_0 + \frac{\mu_1}{137.88}(e^{\lambda T_0} - e^{\lambda T_i}) + \frac{\mu_2}{137.88}(e^{\lambda T_i} - 1) \\ z_i &= z_0 + \mu_1\kappa_1(e^{\lambda''T_0} - e^{\lambda''T_i}) + \mu_2\kappa_2(e^{\lambda''T_i} - 1) \end{aligned} \quad (7)$$

#### THE Pb ISOTOPE TOOLBOX: MODEL AGE $T$ , $\mu$ AND $\kappa$

Equations (7) show that, even for a simple two-stage evolution approximation, Pb isotope ratios in ores depend in a complex way on several *a priori* independent parameters:  $\mu_1$ ,  $\mu_2$ ,  $\kappa_1$ ,  $\kappa_2$  and the *model age*  $T_i$ . Even though Pb isotopic ratios can be used to compare samples, they do not readily allow for the information on the history of the analysed Pb to be read. We will therefore use a

simplifying assumption to show how to extract these parameters, and how to use them to describe the geological and geochemical properties of the metal sources. The simplifying assumption, which goes back several decades, states that most metallic ores are in the form of sulphides, which accommodate large concentrations of Pb but, in nearly every case, have very low U and Th contents. It can therefore safely be assumed that, for sulphides,  $\mu_2 \approx 0$  from  $T_i$  to the present. We will now describe procedures to retrieve  $\mu_i$ ,  $\kappa_i$  and  $T_i$  ( $\kappa_2$  is no longer relevant).

*Pb geological model ages*

We will first show how to derive a model age  $T_i$  for the geological basement using the Pb isotope composition of any given ore with respect to modern upper continental crust.  $T_0$  is the age at which the Earth’s mantle and crust formed, and  $T_i$  is the geological ‘model’ age of ore sample  $i$ . The subscript 0 refers to primordial Pb, and the superscript asterisk (\*) to modern common Pb (Cumming and Richards 1975; Stacey and Kramers 1975; Albarède and Juteau 1984). We define:

$$\Delta\mu_i = \mu_i - \mu^* \tag{8}$$

$$\Delta\kappa_i = \kappa_i - \kappa^* \tag{9}$$

The equations for the two-stage evolution of the U–Pb systems between  $T_0$  and  $T_i$ , with no U being present after that time, are as follows:

$$\begin{aligned} x_i &= x_0 + \mu_i(e^{\lambda T_0} - e^{\lambda T_i}) \\ &= x_0 + \mu^*(e^{\lambda T_0} - 1) - \mu^*(e^{\lambda T_i} - 1) + \Delta\mu_i(e^{\lambda T_0} - e^{\lambda T_i}) \end{aligned} \tag{10}$$

with similar relationships for  $y_i$  and  $z_i$ . A first set of chronometric equations now reads:

$$\begin{aligned} x_i &= x^* - \mu^*(e^{\lambda T_i} - 1) + \Delta\mu_i(e^{\lambda T_0} - e^{\lambda T_i}) \\ y_i &= y^* - \frac{\mu^*}{137.88}(e^{\lambda T_i} - 1) + \frac{\Delta\mu_i}{137.88}(e^{\lambda T_0} - e^{\lambda T_i}) \end{aligned} \tag{11}$$

The geological parameter  $\Delta\mu_i$  is eliminated between the last two equations, to give:

$$f(T_i) = \frac{y_i - y^*}{x_i - x^*} - s(T_0, T_i) - \frac{\mu^*(e^{\lambda T_i} - 1)}{x_i - x^*} [s(T_0, T_i) - s(T_i, 0)] = 0 \tag{12}$$

*The U/Pb of the ore source*

Once  $T_i$  is known, any of the equations (11) will give  $\Delta\mu_i$  and, from equation (9),  $\mu_i$ .

*The Th/U of the ore source*

Likewise,  $\Delta\kappa_i$  of the  $^{232}\text{Th}$ – $^{208}\text{Pb}$  system is computed as follows:

$$z_i = z_0 + \kappa_i\mu_i(e^{\lambda T_0} - e^{\lambda T_i}) = z_0 + (\mu^*\kappa^* + \mu_i\Delta\kappa_i + \kappa^*\Delta\mu_i)(e^{\lambda T_0} - e^{\lambda T_i}) \tag{13}$$

or

$$\begin{aligned}
 z_i &= z_0 + \mu^* \kappa^* (e^{\lambda'' T_0} - 1) - \mu^* \kappa^* (e^{\lambda'' T_i} - 1) + (\mu_i \Delta \kappa_i + \kappa^* \Delta \mu_i) (e^{\lambda'' T_0} - e^{\lambda'' T_i}) \\
 &= z^* - \mu^* \kappa^* (e^{\lambda'' T_i} - 1) + (\mu_i \Delta \kappa_i + \kappa^* \Delta \mu_i) (e^{\lambda'' T_0} - e^{\lambda'' T_i})
 \end{aligned}
 \tag{14}$$

which can be solved as

$$\Delta \kappa_i = \frac{z_i - z^* + \mu^* \kappa^* (e^{\lambda'' T_i} - 1) + (\mu_i \Delta \kappa_i + \kappa^* \Delta \mu_i) (e^{\lambda'' T_0} - e^{\lambda'' T_i})}{\mu_i (e^{\lambda'' T_0} - e^{\lambda'' T_i})}
 \tag{15}$$

### Error propagation

The sensitivity of the model age  $T_i$  with respect to a particular choice of  $T_0$  can be obtained by differentiating equations (10) with respect to  $T_0$ ,  $T_i$  and  $\Delta \mu_i$ , and can be shown to be as follows:

$$dT_i = \frac{\Delta \mu_i}{\mu_i} \frac{\lambda' e^{\lambda' T_0} - 137.88 \lambda_s(T_0, T_i) e^{\lambda' T_0}}{\lambda' e^{\lambda' T_i} - 137.88 \lambda_s(T_0, T_i) e^{\lambda' T_i}} dT_0
 \tag{16}$$

### Reference models

Equation (12) is solved for  $T_i$  using the Excel Solver or an in-house Matlab code, which may be obtained from the first author upon request. Parameters used in the various equations are  $\lambda = 0.155125 \times 10^{-9} \text{ a}^{-1}$ ,  $\lambda' = 0.98485 \times 10^{-9} \text{ a}^{-1}$ ,  $\lambda'' = 0.049475 \times 10^{-9} \text{ a}^{-1}$ ,  $T_0 = 4.43 \text{ Ga}$ ,  $x^* = 18.750$ ,  $y^* = 15.63$ ,  $z^* = 38.83$ ,  $\mu^* = 9.66$  and  $\kappa^* = 3.90$  (Stacey and Kramers 1975; Albarède and Juteau 1984).

Alternative modern Pb compositions and models of Pb isotope evolution have been used, notably one based on the assumption that  $\mu$  in the terrestrial mantle increases linearly with time (Cumming and Richards 1975). The geochemical motivations for this model, other than providing an alternative good fit to Pb isotope data on galenas of different ages, are not compelling. In addition, Albarède and Juteau (1984) analysed the evolution of the three chronometric systems individually and were able to show that, within errors and over the last 3.8 Ga, both the  $^{238}\text{U}$ – $^{206}\text{Pb}$  and  $^{235}\text{U}$ – $^{207}\text{Pb}$  chronometers indicate indistinguishable but constant  $\mu$  values consistent with the assumptions of Stacey and Kramers (1975). The present calculation scheme reduces differences in model ages resulting from using different modern Pb to a few tens of Ma for samples younger than 1000 Ma, which is ample precision for archaeometric purposes.

The use of a standard reference model of Pb isotope evolution does not take the existence of non-exhalative, aquifer-related ores with model ages inconsistent with local tectonic ages into account. Such anomalous Pb deposits are best represented by Mississippi Valley ore deposits (Doe and Delevaux 1972), in which recent input of highly radiogenic Pb was assigned to leaching of detrital rocks by the local aquifer. Mississippi Valley type ores are, however, not commonly associated with coinage metal deposits.

### Application to rock samples

When the model age is calculated for Pb in modern volcanic rocks, which can be useful to assess the geological context of ore deposits, the two-stage approximation no longer holds, and what is

obtained is whether the Pb isotope evolution has been accelerated or held back by U/Pb ratios higher (or lower) than those of typical continental crust. Interpreting the 'delay' in terms of a two-stage age requires some assumptions about the second-stage value  $\mu_2$ , which the example below will help clarify.

#### MAPPING THE CENTRAL ANDES WITH Pb ISOTOPES

Spanish America was for centuries a major source of silver (e.g., Potosi, Zacatecas and Cerro de Pasco) and gold for European economies. The abundance of Pb isotope data accumulated over decades for both ore deposits and magmatic rocks in the Central Andes (for a review, see Mamani *et al.* 2008) makes this region an excellent example of how to extract geochemically meaningful information from Pb isotope compositions of archaeological artefacts. The geology of the Central Andes, where most of the silver ore deposits mined in the 16th–18th centuries are located, is summarized by Jaillard *et al.* (2000), Ramos (2000) and Ramos and Aleman (2000). A modern review of the economic geology and relevant literature is given by Mamani *et al.* (2008), who also built a broadly distributed database for Pb isotopes in ore deposits and volcanic rocks.

The geology of the Central Andes can be summarized briefly as follows (Fig. 1 (a)). From east to west, the Eastern Cordillera is the oldest relevant fold belt, which affected geological sedimentary rocks older than 300 Ma (Jacobshagen *et al.* 2002; Haerberlin *et al.* 2004). It is thrust against the Brazilian Precambrian foreland (craton) and is known for major Au–Ag deposits that have been mined since pre-colonial times. It is separated from the Western Cordillera by the Altiplano plateau with its long chain of active and recent volcanoes. The Western Cordillera itself was erected in a series of tectonic phases starting in the late Jurassic (~135 Ma) and lasting virtually up to the present time. Most of these compressional phases are associated with magmatic activity and hydrothermal ore deposits. An extraordinary geological feature is the presence under most of the Northern Altiplano of massive amounts of Palaeozoic and Proterozoic rocks (up to ~2000 Ma old) (Dalmayrac *et al.* 1977; Shackleton *et al.* 1979; Wörner *et al.* 2000), which extend towards the north-west in coastal Peru, where it is intruded by ~390 Ma old magmatic rocks (Mukasa and Henry 1990). These geological formations, known as the Arequipa block, correspond to a particularly thick crust (Lloyd *et al.* 2010), which, as we will see below, imparts a strong imprint on the Pb isotope compositions of ores and magmatic rocks.

The Pb model ages calculated from the database of Mamani *et al.* (2008) reflect this geological arrangement remarkably closely (Fig. 1 (b)). Most magmatic rocks have Pb model ages < 150 Ma, which attest to their emplacement at the time when the Western Cordillera was forming, except for the Altiplano–Arequipa volcanics, which have model ages up to 500 Ma. Such old ages indicate a significant 'delay' in radiogenic Pb ingrowth, which is associated with the presence of the above-mentioned underlying Precambrian and Palaeozoic geological formations, where continental crust is particularly thick and U has been preferentially removed during orogenic events. The ore deposits show a consistent picture, with young Pb model ages in the Western Cordillera, but with a clear contribution from older Pb visible at some localities where the Precambrian basement is near the surface, such as on the northeastern edge of the Altiplano (San Antonio del Nuevo Mondo, Potosi, Oruro).

The  $^{238}\text{U}/^{204}\text{Pb}$  ( $\mu$ , Fig. 1 (c)) and  $^{232}\text{Th}/^{238}\text{U}$  ( $\kappa$ , Fig. 1 (d)) ratios also define geologically meaningful arrangements. The Eastern Cordillera shows slightly higher values (9.75–9.85) than the Altiplano and the Western Cordillera (9.60–9.70). Likewise, the Altiplano and its northwestern coastal extension, both underlain by Precambrian and Palaeozoic geological formations, stand out by virtue of their higher  $\kappa$  values (4.0–4.2) relative to the rest of the area (3.7–3.9). The

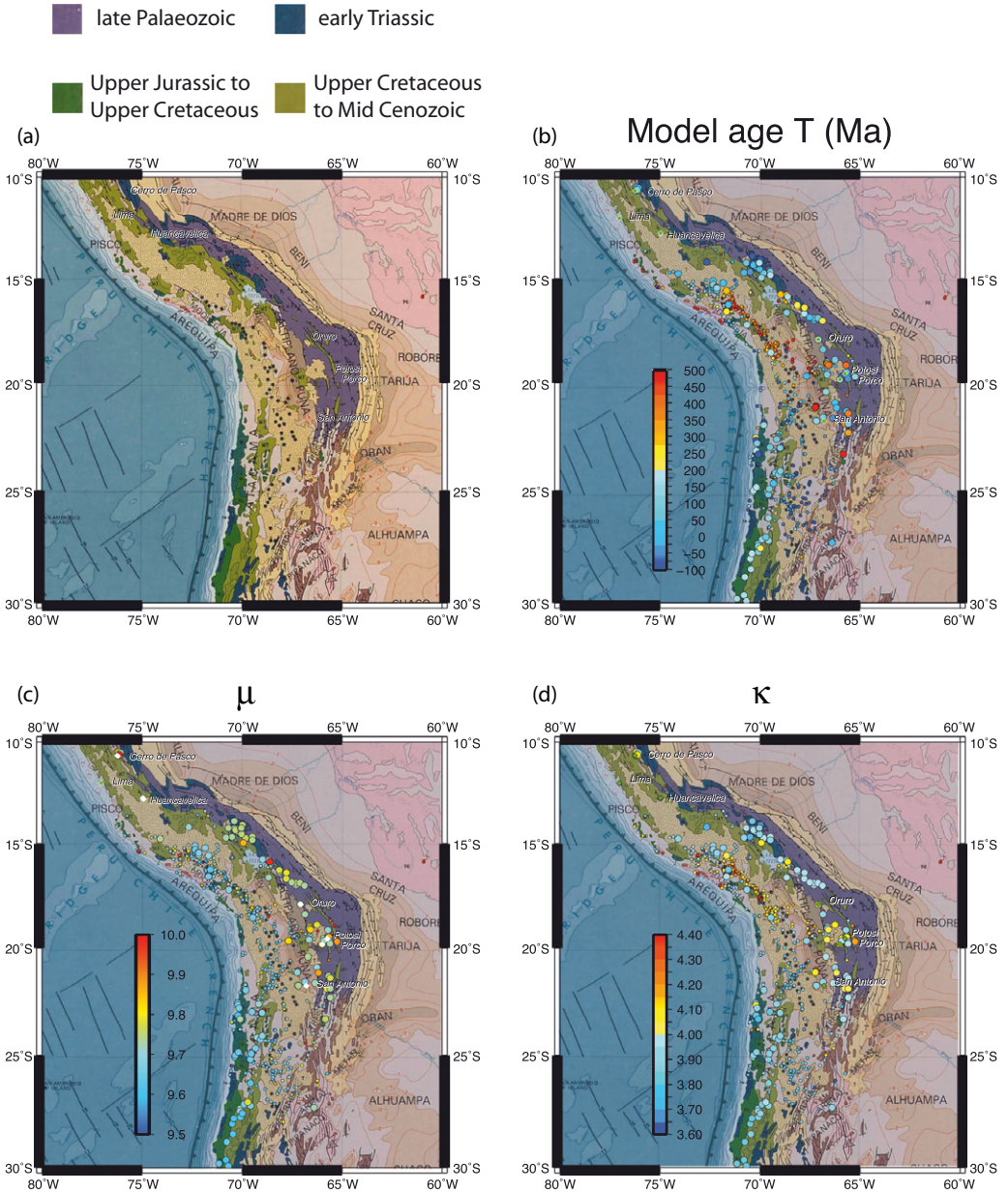


Figure 1 A comparison of model ages,  $^{238}\text{U}/^{204}\text{Pb}$  ( $\mu$ ) and  $^{232}\text{Th}/^{238}\text{U}$  ( $\kappa$ ), calculated for the Pb isotope compositions of Central Andean rocks listed in the database of Mamani et al. (2008) with the geological age of the host province. Large symbols, ore deposits; small symbols, volcanic rocks. (a) The geology of the Central Andes from the Exxon Tectonic Map of the World, showing the tectonic age of the various crustal segments. (pink, Archean and Proterozoic; stars, active volcanoes); (b) model ages, in millions of years (Ma), calculated from equation (12); (c)  $\mu$  and (d)  $\kappa$  values (see online for a colour version of this figure).

highly productive mining districts of Potosi, Porco and San Antonio del Nuevo Mondo, interestingly, are part of the high- $\kappa$  ore deposits.

Although simply plotting raw Pb isotope ratios on the same map also clearly displays some geographical and geological systematics (Mamani *et al.* 2008), the patterns of model ages and  $\mu$  and  $\kappa$  values lend themselves to a stronger and more intelligible geological analysis of provenance. The examples below will illustrate this point.

#### LEAD ISOTOPES IN POTOSI AND MEXICAN SILVER

The Pb isotope data used for this case study are those of 16th–18th century silver coins from the work by Desaulty *et al.* (2011). Figure 2 shows a good consistency of isotopic ratios in coinage and in local ores, with the coinage data demonstrating the averaging effect of metallurgical processing. The model ages,  $\mu$  and  $\kappa$  for these samples are plotted in Figures 3 and 4. The coins were minted in Mexico and South America, mostly at Potosi. The place and date of minting are distinctly identifiable on each coin. Clearly, the Pb isotope compositions of the coins reflect those of the ores. Lead isotope compositions have been measured in most Mexican ore deposits (Cumming *et al.* 1979), but unfortunately with poor localization. Nevertheless, the Mexican ore data are extremely consistent: the model ages ( $20 \pm 70$  Ma) and the  $\mu$  ( $9.67 \pm 0.03$ ) and  $\kappa$

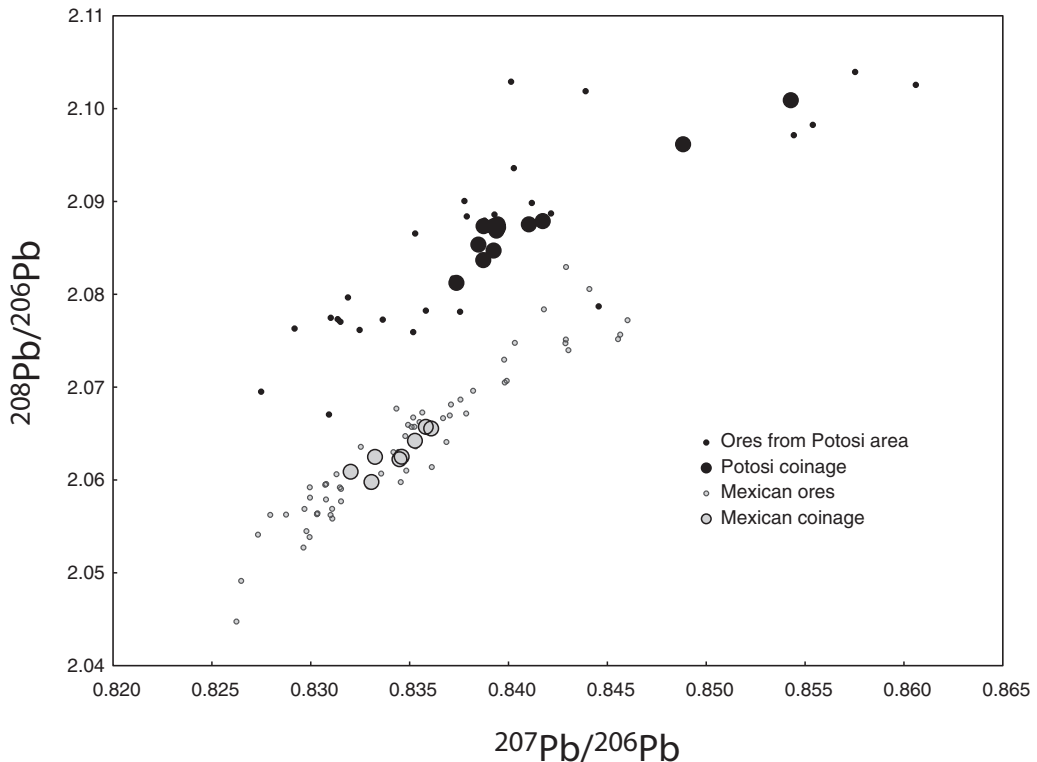


Figure 2 A comparison of  $^{208}\text{Pb}/^{206}\text{Pb}$  and  $^{207}\text{Pb}/^{206}\text{Pb}$  in 16th–18th century coins minted in Potosi and Mexico, as measured by Desaulty *et al.* (2011), and in ores from the Potosi region and Mexico. Data for the Potosi region from Kamenov *et al.* (2002), and for Mexico from Cumming *et al.* (1979).

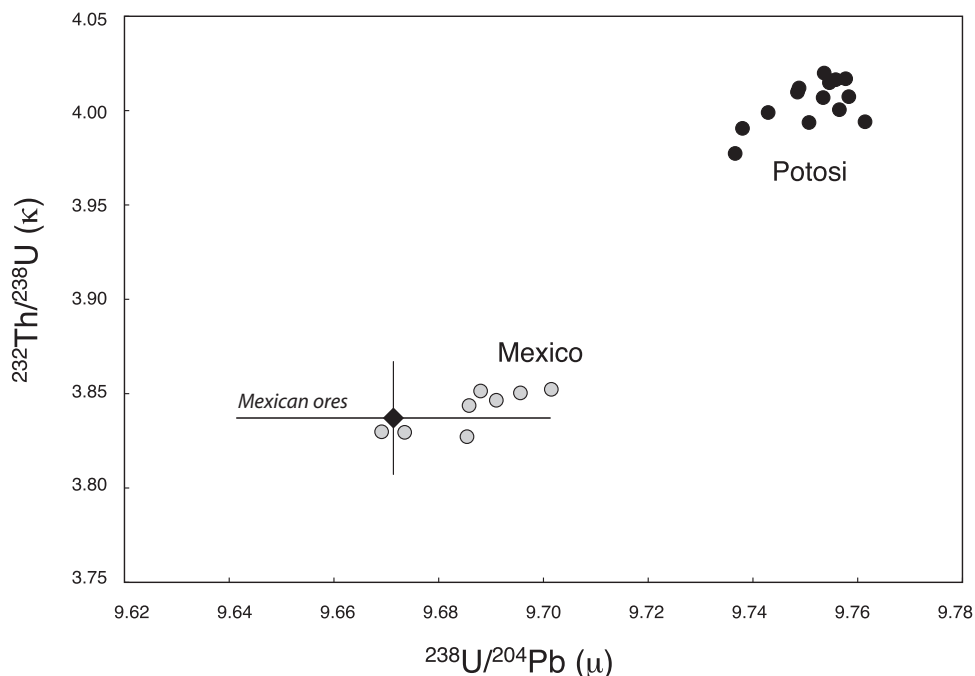


Figure 3 The 16th–18th century coins minted in Potosi and Mexico are clearly distinguishable by their  $^{238}\text{U}/^{204}\text{Pb}$  ( $\mu$ ) and  $^{232}\text{Th}/^{238}\text{U}$  ( $\kappa$ ) values as calculated from the Pb isotope data of Desaulty *et al.* (2011). The solid diamond symbol represents the mean values of  $\mu$  and  $\kappa$  calculated for Mexican ores using the data by Cumming *et al.* (1979). The error bars represent the 95% dispersion of the data. The scatter of Pb isotopic compositions of ores from the Potosi region is large (Fig. 2) and is not shown in this figure. Lead isotopes in historical Potosi silver ores have apparently not been measured, but the available data on the Cerro de Potosi volcanics, although covering a fairly large range of  $T$ ,  $\mu$  and  $\kappa$  (Kamenov *et al.* 2002), are consistent with the Pb isotope compositions of Potosi coins.

( $3.84 \pm 0.03$ ) values are closely grouped, and very different from the ranges for the mining districts of the Central Andes quoted in the previous section. Mexico can therefore be defined as a very young, low- $\mu$  and low- $\kappa$  lead isotope province, whereas Peru–Bolivia has Cordilleran ages or older with high  $\mu$  and high  $\kappa$ . Lead isotopes in historical Potosi silver ores have apparently not been measured so far, but the available data on the Cerro de Potosi volcanics, sulphides and sediments, although covering a fairly large range of  $T$ ,  $\mu$  and  $\kappa$  (Kamenov *et al.* 2002), with model ages ranging from 170 to 600 Ma and mean values of  $\mu = 9.76 \pm 0.09$  and  $\kappa = 4.07 \pm 0.06$ , are fully consistent with the Pb isotope compositions of Potosi coins. The reliability of this approach for assigning provenance to silver of a particular coinage hence appears extremely good. As shown by Desaulty *et al.* (2011), such fingerprinting of American Pb in coinage enhances information on provenance obtained from the stable isotopes of Cu and Ag, and is particularly helpful in assessing the fluxes of silver through the individual European economies.

#### THE RECONQUISTA OF SOUTHERN SPAIN

By the middle of the 15th century, the last Arab stronghold in Spain was the Emirate of Granada, which was home to major silver mines that had been exploited since the Carthaginian and Roman times. The major silver mines of southern Spain belong to geological formations that were last

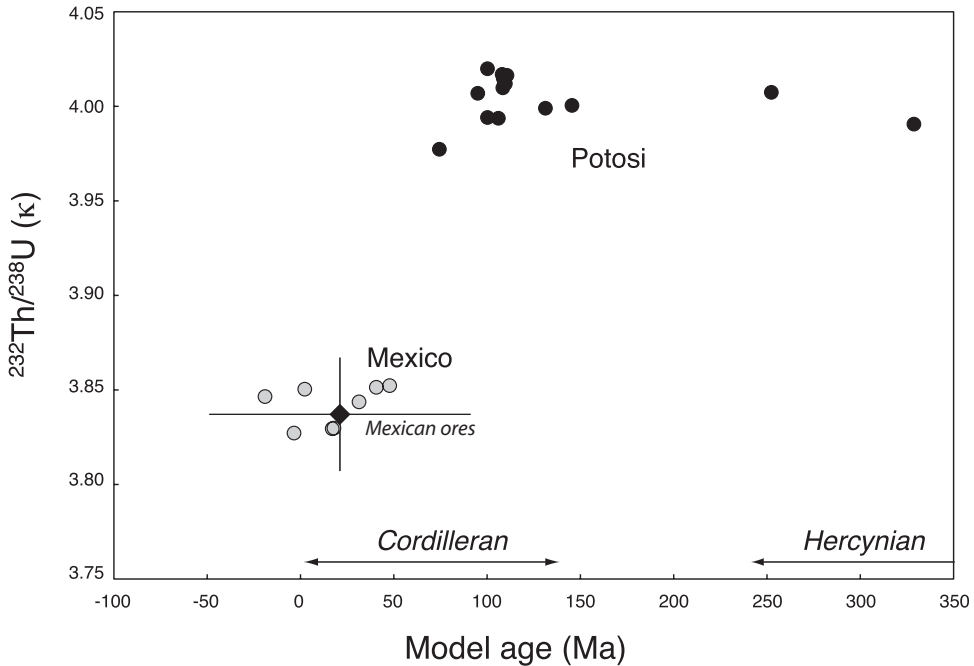


Figure 4 The 16th–18th century coins minted in Potosi and Mexico also can be distinguished when using their Pb model ages and  $^{232}\text{Th}/^{238}\text{U}$  ( $\kappa$ ) values calculated from the Pb isotope data of Desaulty *et al.* (2011). The solid diamond symbol represents the mean values of the Pb model age and  $\kappa$  calculated for Mexican ores measured by Cumming *et al.* (1979). The error bars represent the 95% dispersion of the data. The model ages of Potosi coins are substantially older (Jurassic to Cretaceous) than the model ages of Mexican coins (Cenozoic). A contribution of Pb from an old basement is visible at Potosi.

reworked within the Betic fold belt some 20 My ago. After the Ottomans overran Kosovo and Serbia and their Oligocene mines in 1463 (Pamuk 2000), the most productive mines remaining in European hands before the expansion of the Spaniards in South and Central America were those of Saxony (Freiberg, Schneeberg) and the Tyrol (Schwarz), which were hosted in Late Palaeozoic (~300 Ma old) formations (Nef 1941; Dill *et al.* 2008). Old model ages are expected—and found—in Pb from the West European silver coins produced in the late 15th and early 16th centuries. Spanish coins are an interesting exception.

Of all the medieval silver coins for which Desaulty *et al.* (2011) analysed Pb isotopes, only those dated from the Catholic Monarchs Ferdinand of Aragon and Isabella of Castile, who jointly ruled Spain from 1479 to 1516, present young, non-Hercynian Pb model ages < 100 Ma (Fig. 5). This can be understood with reference to the capture by the Catholic Monarchs of the Emirate of Granada, which began in 1482 and was complete by 1491. The seizure of the rich silver mines of the Cartagena–Almeria volcanic belt in the Betic realm (Oen *et al.* 1975; Lunar *et al.* 2002) distinctly shows up in the Pb isotopes of the Spanish coins of that time (Fig. 6). This example illustrates how useful inferences can be made from Pb isotope compositions about the provenance of metals without the need to make actual measurements on specific ores.

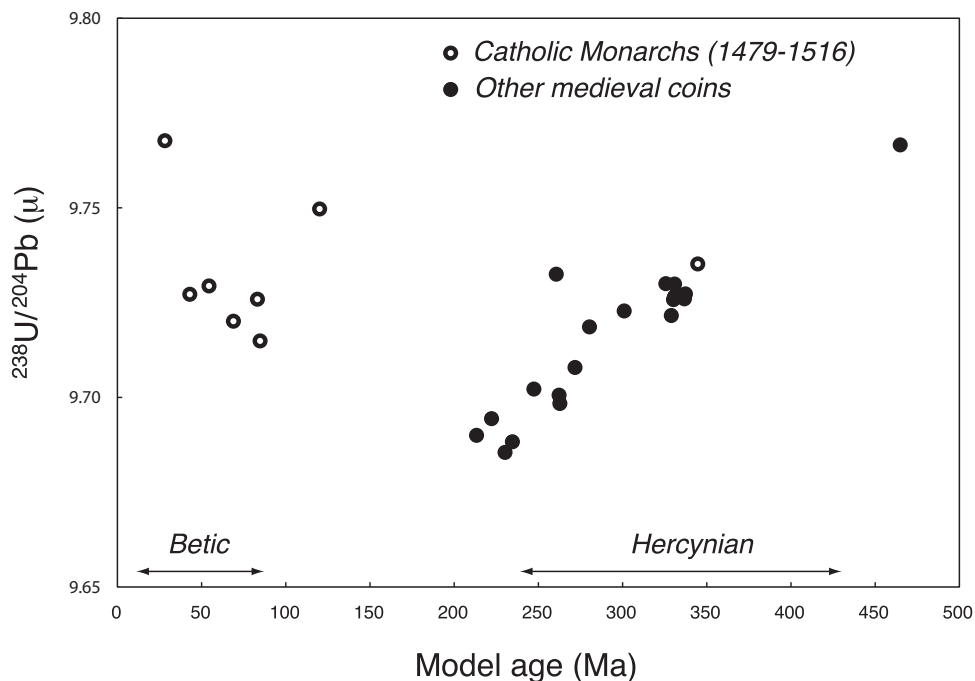


Figure 5 Lead model ages of various silver coins from medieval Europe and Spain at the time of the Catholic Monarchs (Desaulty et al., 2011). All but one of the Catholic Monarchs coins have young model ages, indicating that the source of lead (and, hence, presumably also of silver) lies in a young geological province that can be identified as the Betic terranes of the Emirate of Granada. The rest of the coins have Hercynian Pb model ages and, therefore, sources in mainland Europe, probably in Saxony or the Tyrol.

#### CONCLUDING REMARKS

Much has been said about the potential of Pb isotopes to discriminate metal from different provenances and much has been written about Pb isotope modelling. The combination of the two, however, remains largely unexploited and the present work has attempted to fill this gap by showing how a geologically informed assessment of provenance may be obtained even in the absence of detailed isotopic information on potential source ores. Expressions have been laid out for the calculation of Pb model ages and U/Pb and Th/U ratios of metal sources. An example of how to apply these theoretical concepts to a given geological context is provided by the Central Andes, which illustrates how geochemical mapping of the parameters extracted from Pb isotope compositions can pertain to a province with abundant mines. Two case studies, one dealing with the distinction between Mexican and Andean ores, and another showing how the Reconquista 'reads' in Pb from silver coins, further demonstrate the potential of this method.

#### ACKNOWLEDGEMENTS

We thank the Institut National des Sciences de l'Univers and the Ecole Normale Supérieure for financial support. We are particularly grateful to Jacques Samarut, Chantal Rabourdin-Combes, Dominique Le Quéau and Mireille Perrin for their encouragement. Funding by the Région

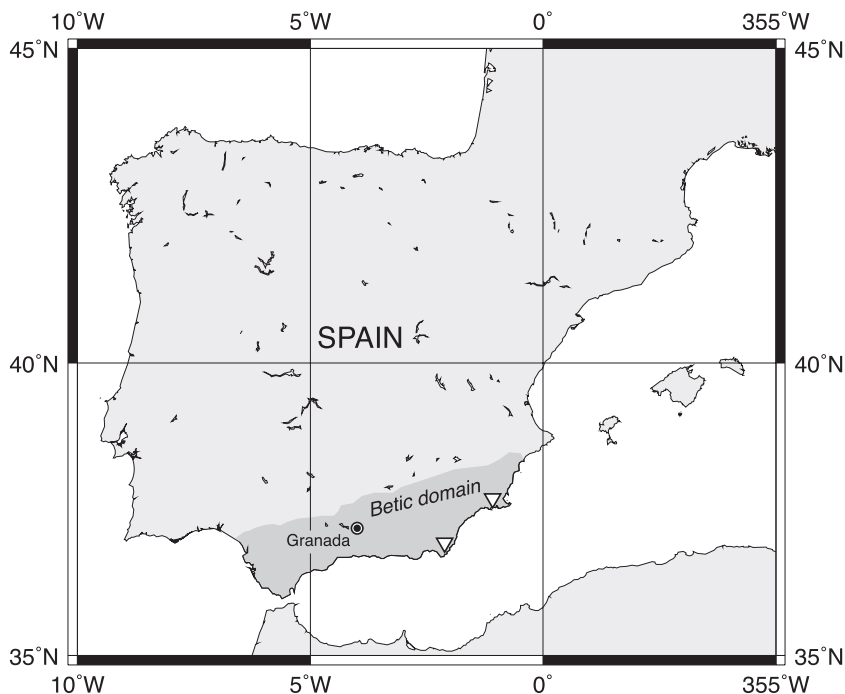


Figure 6 The Betic domain (dark grey), which formed some 20 My ago, occupies the southern part of the Iberian Peninsula. The rest of Spain (except for the Pyrenees) formed during Hercynian times (400–250 My ago). Triangles represent major silver mines.

Rhône-Alpes programme CIBLES was particularly helpful. We are also grateful to Gerhard Wörner for sharing his Pb isotope database of the Andes, and to Bert Bally for sharing his copy of the Exxon Tectonic Map of the World. The Department of Earth Science and the Wiess Foundation of Rice University greatly facilitated our completion of this work. The three anonymous reviewers helped clarify the relationship between the standard use of isotopic plots in archaeometry and the method presented here.

#### REFERENCES

- Albarède, F., and Juteau, M., 1984, Unscrambling the lead model ages, *Geochimica Cosmochimica Acta*, **48**, 207–12.
- Allègre, C. J., 2008, *Isotope geology*, Cambridge University Press, Cambridge, UK.
- Baker, J., Stos, S., and Waight, T., 2005, Lead isotope analysis of archaeological metals by multiple-collector inductively coupled plasma mass spectrometry, *Archaeometry*, **48**, 45–56.
- Bielicki, K. H., and Tischendorf, G., 1991, Lead isotope and Pb–Pb model age determinations of ores from Central Europe and their metallogenetic interpretation, *Contributions to Mineralogy and Petrology*, **106**, 440–61.
- Blichert-Toft, J., Agranier, A., Andres, M., Kingsley, R., Schilling, J. G., and Albarède, F., 2005, Geochemical segmentation of the Mid-Atlantic Ridge north of Iceland and ridge–hot spot interaction in the North Atlantic, *Geochemistry, Geophysics, Geosystems*, **6**, Q01E19.
- Cattin, F., Villa, I. M., and Besse, M., 2009, Copper supply during the Final Neolithic at the Saint-Blaise/Bains des Dames site (Neuchâtel, Switzerland), *Archaeological and Anthropological Sciences*, **1**, 161–76.
- Cumming, G. L., and Richards, J. R., 1975, Ore lead isotope ratios in a continuously changing earth, *Earth and Planetary Science Letters*, **28**, 155–71.

- Cumming, G. L., Kesler, S. E., and Krstic, D., 1979, Isotopic composition of lead in Mexican mineral deposits, *Economic Geology*, **74**, 1395–407.
- Dalmayrac, C., Lancelot, J., and Leyreloup, A., 1977, Evidence of 2 b.y. granulites in the late Precambrian metamorphic basement rocks along the southern Peruvian coast, *Science*, **198**, 49–51.
- Desaulty, A. M., Telouk, P., Albalat, E., and Albarède, F., 2011, The isotopic Ag–Cu–Pb record of silver circulation through 16–18th century Spain, *Proceedings of the National Academy of Sciences*, **108**, 9002–7.
- Dickin, A. P., 2005, *Radiogenic isotope geology*, Cambridge University Press, Cambridge, UK.
- Dill, H. G., Sachsenhofer, R. F., Grecula, P., Sasvári, T., Palinkaš, L. A., Borojević-Šoštarić, S., Strmić-Palinkaš, S., Prochaska, W., Garuti, G., Zaccarini, F., Arbouille, D., and Schulz, H.-M., 2008, Fossil fuels, ore and industrial minerals, in *The geology of Central Europe* (ed. T. McCann), The Geological Society, London.
- Doe, B. R., and Delevaux, M. I.-I., 1972, Source of lead in southeast Missouri galena ores, *Economic Geology*, **67**, 409–25.
- Elliott, T., Zindler, A., and Bourdon, B., 1999, Exploring the kappa conundrum: the role of recycling in the lead isotope evolution of the mantle, *Earth and Planetary Science Letters*, **169**, 129–45.
- Gale, N. H., 1972, Uranium–lead systematics in lunar basalts, *Earth and Planetary Science Letters*, **17**, 65–78.
- Gordus, A. A., and Gordus, J. P., 1981, Potosi silver and coinage of early modern Europe, in *Precious metals in the age of expansion* (ed. H. Kellenbenz), 225–41, Klett-Cotta, Stuttgart.
- Haeblerlin, Y., Moritz, R., Fontboté, L., and Cosca, M., 2004, Carboniferous orogenic gold deposits at Patataz, Eastern Andean Cordillera, Peru: geological and structural framework, paragenesis, alteration, and  $^{40}\text{Ar}/^{39}\text{Ar}$  geochronology, *Economic Geology*, **99**, 73–112.
- Jacobshagen, V., Müller, J., Wemmer, K., Ahrendt, K. H., and Manutsoglu, E., 2002, Hercynian deformation and metamorphism in the Cordillera Oriental of southern Bolivia, Central Andes, *Tectonophysics*, **345**, 119–30.
- Jaillard, E., Hérail, I. G., Monfret, T., Diaz-Martínez, E., Baby, P., Lavenue, A., and Dumont, J.-F., 2000, Tectonic evolution of the Andes of Ecuador, Peru, Bolivia, in *Tectonic evolution of South America* (eds. U. G. Cordani, E. J. Milani, A. Thomas Filho and D. A. Campos), 31st International Geological Congress, Rio de Janeiro.
- Kamenov, G., Macfarlane, A. W., and Riciputi, L., 2002, Sources of lead in the San Cristobal, Pulacayo, and Potosi mining districts, Bolivia, and a reevaluation of regional ore lead isotope provinces, *Economic Geology*, **97**, 573–92.
- Klein, S., Lahaye, Y., Brey, G. P., and Von Kaenel, H.-M., 2004, The early Roman imperial AES coinage II: tracing the copper sources by analysis of lead and copper isotopes—copper coins of Augustus and Tiberius, *Archaeometry*, **46**, 469–80.
- Le Roy Ladurie, E., Barrandon, J.-N., Collin, B., Guerra, M.-F., and Morrisson, C., 1990, Sur les traces de l'argent du Potosi, *Annales ESC*, **2**, 483–505.
- Lloyd, S., Van Der Lee, S., França, G. S., Assumpção, M., and Feng, M., 2010, Moho map of South America from receiver functions and surface waves, *Journal of Geophysical Research*, **115**, doi:10.1029/2009JB006829.
- Lunar, R., Moreno, T., Lombardero, M., Regueiro, M., Lopez-Vera, F., Martínez del Olmo, W., Mallo García, J. M., Saenz de Santa María, J. A., Carcia-Palomero, F., Higuera, P., Ortega, L., and Capote, R., 2002, Economic and environmental geology, in *The geology of Spain* (eds. W. Gibbons and T. Moreno), 473–510, The Geological Society, London.
- Mamani, M., Tassara, A., and Wörner, G., 2008, Composition and structural control of crustal domains in the Central Andes, *Geochemistry, Geophysics, Geosystems*, **9**, doi:10.1029/2007GC001925.
- Michard-Vitrac, A., Albarède, F., and Allègre, C. J., 1981, Lead isotopic composition of Hercynian granitic K-feldspars constrains continental genesis, *Nature*, **291**, 460–4.
- Mukasa, S. B., and Henry, D. J., 1990, The San Nicolas batholith of coastal Peru: early Palaeozoic continental arc or continental rift magmatism? *Journal of the Geological Society of London*, **147**, 27–39.
- Nef, J. U., 1941, Silver production in Central Europe, *The Journal of Political Economy*, **49**, 575–91.
- Oen, I. S., Fernandez, J. C., and Manteca, J. I., 1975, The lead–zinc and associated ores of La Union, Sierra de Cartagena, Spain, *Economic Geology*, **70**, 1259–78.
- Oversby, V. M., and Gast, P. W., 1968, Oceanic basalt leads and the age of the Earth, *Science*, **162**, 925–7.
- Pamuk, S., 2000, *A monetary history of the Ottoman Empire*, Cambridge University Press, Cambridge.
- Pernicka, E., Begemann, F., Schmitt-Strecker, S., and Wagner, G. A., 1993, Eneolithic and Early Bronze Age copper artefacts from the Balkans and their relation to Serbian copper ores, *Praehistorisches Zeitschrift*, **68**, 1–54.
- Pollard, A. M., 2008, Lead isotope geochemistry and the trade in metals, in *Archaeological chemistry*, 2nd edn (eds. A. M. Pollard and C. Heron), 302–45, The Royal Society of Chemistry, London.
- Ponting, M., Evans, J. A., and Pashley, V., 2003, Fingerprinting of Roman mints using laser ablation MC–ICP–MS lead isotope analysis, *Archaeometry*, **4**, 591–7.

- Ramos, V. A., 2000, The southern Central Andes, in *Tectonic evolution of South America* (eds. U. G. Cordani, E. J. Milani, A. Thomas Filho and D. A. Campos), 561–604, 31st International Geological Congress, Rio de Janeiro.
- Ramos, V. A., and Aleman, A., 2000, Tectonic evolution of the Andes, in *Tectonic evolution of South America* (eds. U. G. Cordani, E. J. Milani, A. Thomas Filho and D. A. Campos), 535–85, 31st International Geological Congress, Rio de Janeiro.
- Shackleton, R. M., Ries, A. C., Coward, M. P., and Cobbold, P. R., 1979, Structure, metamorphism and geochronology of the Arequipa Massif of coastal Peru, *Journal of the Geological Society of London*, **136**, 195–214.
- Stacey, J. S., and Kramers, J. D., 1975, Approximation of terrestrial lead isotope evolution by a two-stage model, *Earth and Planetary Science Letters*, **26**, 207–21.
- Stos-Gale, Z. A., 2001, The impact of natural sciences on studies of hacksilber and early silver coinage, in *Hacksilber to coinage: new insights into the monetary history of the Near East and Greece* (ed. M. S. Balmuth), 53–76, American Numismatic Society, New York.
- Stos-Gale, Z. A., and Gale, N. H., 2009, Metal provenancing using isotopes and the Oxford archaeological lead isotope database (OXALID), *Archaeological and Anthropological Sciences*, **1**, 195–213.
- Stos-Gale, Z. A., Gale, N., Houghton, J., and Speakman, R., 1995, Lead isotope data from the Isotrace Laboratory, Oxford: *Archaeometry* data base 1, ores from the western Mediterranean, *Archaeometry*, **37**, 407–15.
- Tera, F., and Wasserburg, G. J., 1972, U–Th–Pb systematics in three Apollo 14 basalts and the problem of initial Pb in lunar rocks, *Earth and Planetary Science Letters*, **14**, 281–304.
- Tera, F., and Wasserburg, G. J., 1973, A response to a comment on U–Pb systematics in lunar basalts, *Earth and Planetary Science Letters*, **19**, 213–17.
- Ulrych, T. J., 1967, Oceanic basalt leads: a new interpretation and an independent age for the Earth, *Science*, **158**, 252–6.
- Wörner, G., Lezauna, J., Becka, A., Hebera, V., Lucassen, F., Zinngrebe, E., Rössling, R., and Wilke, H. G., 2000, Precambrian and Early Paleozoic evolution of the Andean basement at Belen (northern Chile) and Cerro Uyarani (western Bolivia Altiplano), *Journal of South American Earth Sciences*, **13**, 717–37.